A Study on Different Topologies of the Tubular Linear Permanent Magnet Motor Designed for Linear Reciprocating Compressor Applications

Izzeldin I. Abdalla, Taib B. Ibrahim, and Nursyarizal M. Nor

Department of Electrical and Electronic Engineering
Universiti Teknologi PETRONAS, Bandar Seri Iskandar, Perak Darul Ridzuan 32610, Malaysia
izzeldin_abdalla@yahoo.com, taibib@petronas.com.my, nursyarizal_mnor@petronas.com.my

Abstract **─** This paper presents a study on three different topologies of tubular linear permanent magnet motors (TLPMMs), with different permanent magnet (PM) structures. These motors provide direct conversion for electrical energy into a linear mechanical force, and they are directly coupled to the load. The proposed motors are equipped with quasi-Halbach magnetized moving-magnet armatures and their stator cores have been made from a soft magnetic composite (SMC) material, Somaloy 700. Based on the nonlinear time-stepping two-dimensional finite-element analysis (2-D FEA) an extensive magnetic field analysis of the proposed designs has been established. The simulation results indicate the effectiveness of the designs to drive a linear reciprocating compressor in a household refrigerator. Moreover, the simulation results have shown that, the superiority of the two designs with T-shaped and trapezoidal-shaped PMs structures over the TLPMM with conventional rectangular-shaped PMs. In addition to that, the usage of quasi-Halbach for the PMs array arrangement has a significant effect on the motor performance.

Index Terms **─** Finite-element analysis, magnetic field distribution, quasi-Halbach, soft magnetic composite material, tubular linear permanent magnet motor.

I. INTRODUCTION

Linear electromagnetic motors, which can provide a thrust force directly to a payload without any mechanical conversion means, are dedicated to widespread applications, ranging from transportation and industrial automation to healthcare and linear reciprocating compressors. Of the various linear electromagnetic motor topologies, the tubular linear permanent magnet motors (TLPMMs) with a moving-magnet are particularly attractive as compared with their flat counterparts. Because TLPMMs possess a high efficiency and high thrust force capability [1,2].

At present, the energy technologies have significant effects in a social grade of living and economic construction at all scales. This will put further pressure on energy supplies and necessitate energy conservation measures. Meanwhile, the impact of carbon and carbon dioxide (CO_2) emissions based on the Kyoto protocol has increased the major concern of the researchers [3,4].

The refrigerators represent a considerable and growing electrical load [5]. Undoubtedly, among refrigeration devices, the household refrigerator is the most important appliance in our lives today. In the fact that, the household refrigerator uses chlorofluoro-carbons (CFCs) in its installation foam, it contributes to the global warming and ozone layer depletion. It also has a significant impact on the emission of carbon and CO_2. Moreover, while the electrical energy consumption of the individual household refrigerator is small, large numbers of household refrigerators have an appreciable potential on energy consumption. In addition to that, the mechanical friction of the crank-driven piston uses the concept of rotary-to-linear movement in the compressor of the conventional refrigerator. This friction lowers the performance of the refrigerator, and also, the side force between the piston and cylinder lowers the smoothness of the operation system. All these problems are due to the inefficient reciprocating compressor system [6-9].

The conventional rotary reciprocating compressor comprises a single-phase rotary induction motor integrated with a crank as well as a reciprocating piston. The overall efficiency of the compressor is relatively low; this is due to the low efficiency of the induction motor and the mechanical friction of the crank-driven piston movement [10-12].

To enhance the performance of the conventional compressor, it must eliminate the rotary-to-linear motion mechanical conversion means. This can reduce the volume and complexity of the compressor as well as allow the compressor to operate without lubrication. This results in reducing the cost and the power loss as well as enabling a soft operation system [13].

The design of a linear motor has a significant role on the performance of the linear reciprocating compressor. This paper aims to study the performance and magnetic field distribution of a TLPMM under three different topologies, with different permanent magnet (PM) structures. These designs are proposed to drive a linear

Submitted On: October 16, 2014
Accepted On: October 22, 2015

reciprocating compressor in a household refrigerator. Such designs possess the advantages of high force capability, high efficiency, and low manufacturing cost. Moreover, the cogging force due to the stator slotting is very low. The motors were designed to produce an output power of 185 W at a speed of 2.2 m/s. The PMs have been mounted on a mild steel tube in order to produce a higher air gap field.

II. LINEAR MOTOR DESIGN

The main criteria of the appropriate design for a linear motor are based on the simple structure and reasonable cost as well as force capability. It can be noted that the performance of the TLPMM can be well improved by different PM array structures or PM array arrangements [14]. The three designs with various PM structures are rectangular-shaped PMs (Rec_PMs), T-shaped PMs (TS_PMs) and trapezoidal-shaped PMs (Trap_PMs), which are shown in Fig. 1 (a), (b) and (c), respectively. The three designs are equipped with a quasi-Halbach magnetized moving-magnet armature as indicated in Fig. 1, which is comprised of three radially magnetized magnets and two axially magnetized magnets, as presented in [15]. The air gap has been selected to be as small as mechanically possible, because a large air gap leads to an increasing in the PM volume and a reduction in the motor thrust force. However, a very small air gap results in a mechanical fault, and causes some manufacturing difficulties.

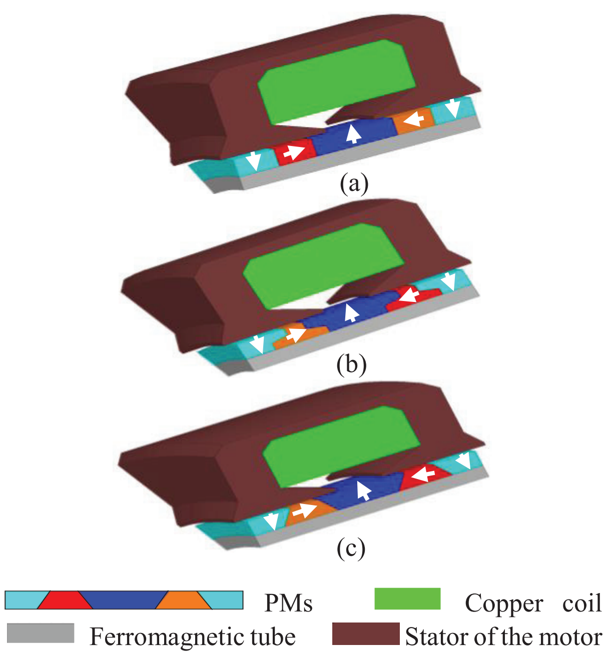

Fig. 1. 3D-FE models of the three proposed TLPMMs with: (a) Rec_PMs, (b) TS_PMs, and (c) Trap_PMs.

The common feature of the three proposed designs is that no field winding is required; only the PMs will generate the excitation field for the motor. Moreover, the stator cores of the three proposed motors are made of soft magnetic composite (SMC) material, Somaloy 700, whereas the PMs are made of rare-earth materials, such as neodymium-iron-boron (NdFeB).

III. LINEAR MOTOR MODEL

The TLPMM can be modeled as follows, the electromagnetic force, $f_e(t)$, of the TLPMM is produced by the interaction between the stator current, i_a and the PMs field. The force can be quantified by [16]:

$$f_e(t) = K_T(x(t))i_a , \quad (1)$$

where the force coefficient, K_T, is slightly position dependent due to the finite armature length. The voltage equation, v_1, associated with the equivalent circuit of the TLPMM in Fig. 2 is as follows:

$$v_1 = R_a i_a + L_s \frac{di_a}{dt} + e_1 , \quad (2)$$

where e_1 is the value of induced electromotive force. The L_s and R_a are the winding inductance and resistance of the motor, respectively [16].

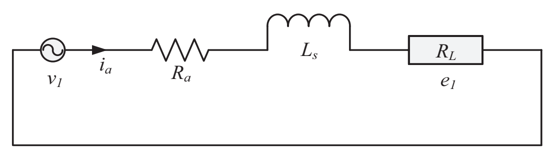

Fig. 2. Equivalent circuit of a single-phase TLPMM.

Faraday's low stated that the magnitude of e_1 is proportional to the rate of change of flux linkage (ψ), which in turn depends on the number of winding turns N_c as:

$$\psi = N_c . \phi . \quad (3)$$

Thus

$$e_1 = \frac{d\psi}{dt} = N_c . \frac{d\phi}{dt} . \quad (4)$$

When the mover is moving along the z-direction, the magnetic field in the stator is static; hence, the distribution of the air gap magnetic field varies with the position of the mover. So, the flux coupled with the winding is varied with time. The induced electromotive force can be rewritten as in (5):

$$e_1 = \frac{d\psi}{dt} = \frac{d\psi}{dz} \times \frac{dz}{dt} = v \times \frac{d\psi}{dz} , \quad (1)$$

where $v = dz/dt$ is the mover velocity along the z-direction. Thus, the back-EMF is given by the product of v, and the rate of change in the flux-linkage, ψ, with respect to the position. The inductance of a winding, L, is given by the ratio between the flux linked with the winding and the current into the winding as expressed in (6) [17]. The magnetization curve of the NdFeB magnet can be expressed as in (7) [18]:

$$L = \psi / i_a , \quad (6)$$

$$B_m = \mu_r H_m + B_r \,, \tag{7}$$

where B_m is the magnetic flux density in axial direction, H_m is the magnetizing force, B_r the magnet remanence, and μ_r is the relative permeability of the magnet.

The following three Maxwell's equations used by the FEA and relevant to magnetic field analysis of the proposed motors. Thus, (11) resulted from (8) and (9):

$$\nabla \times H = -\sigma(E) \,, \tag{8}$$

$$\nabla \times E = -\frac{\partial B}{\partial t} \,, \tag{9}$$

$$\nabla . B = 0 \,, \tag{10}$$

$$\nabla \times \frac{1}{\sigma} \nabla \times H + \frac{\partial B}{\partial t} = 0 \,. \tag{11}$$

The governing field equations of the proposed motors in the cylindrical coordinate system, in terms of the vector magnetic potential (A_θ), are given by (12) for the airspace region and (13) for magnet region:

$$\frac{\partial}{\partial z}\left(\frac{1}{r}\frac{\partial}{\partial z}\left(rA_{I\theta}\right)\right) + \frac{\partial}{\partial r}\left(\frac{1}{r}\frac{\partial}{\partial r}\left(rA_{I\theta}\right)\right) = 0 \,, \tag{12}$$

$$\frac{\partial}{\partial z}\left(\frac{1}{r}\frac{\partial}{\partial z}\left(rA_{(II\theta)}\right)\right) + \frac{\partial}{\partial r}\left(\frac{1}{r}\frac{\partial}{\partial r}\left(rA_{(II\theta)}\right)\right) = -\mu_0 \nabla \times M \,. \tag{13}$$

IV. MAGNETIC FIELD ANALYSIS

The two-dimensional finite-element analysis (2-D FEA), under Ansys Maxwell 16, commercial version has been used to design and analyze the performance of the three proposed TLPMMs. Hence, the transient solver of this software has been used to examine the electromagnetic characteristics of the three proposed designs. Hence, all the results are established in a cylindrical coordinate system. The 2-D FEA presents a significant advantage of being less time consuming as compared with the 3-D FEA. The main parameters of the design are tabulated as in Table 1. The same parameters have been used to build the 2-D axisymmetrical FE models of the three proposed designs.

Table 1: Design parameters

The Parameter	Symbol	Value
Outer radius of the stator core	R_e	50.0 mm
Yoke thickness	h_{ys}	3.3 mm
Outer radius of the magnet	R_m	20.0 mm
Magnet height	h_m	5.0 mm
Air gap length	g	0.8 mm
Tooth width	T_w	9.4 mm
Slot opening width	b_0	10.0 mm
Tooth tip height	h_t	1.0 mm
Magnet remanence	B_r	1.14 T
Length of the radial PM	T_{mr}	15.5 mm
Length of the axial magnet	T_{mz}	9.5 mm
Ferromagnetic height	h_{ym}	3.9 mm
Tooth pitch width	T_w	40 mm
Pole pitch	T_p	25 mm

Figure 3 illustrates the linear B-H curve of the NdFeB, PMs and the nonlinear B-H curve of the SMC material, Somaloy 700, which have been used in the 2-D FEA solution. Basically, the characteristics of the PMs are described by the following quantities: coercive force, H_c; relative permeability, μ_r; remanence, B_r; as well as chemical characteristics and the second quarter of the hysteresis loop [19]. In the FEA calculations, the material linearity of the NdFeB PMs has been included, such as H_C = -864 kA/m, μ_r = 1.05 and B_r = 1.14 Tesla.

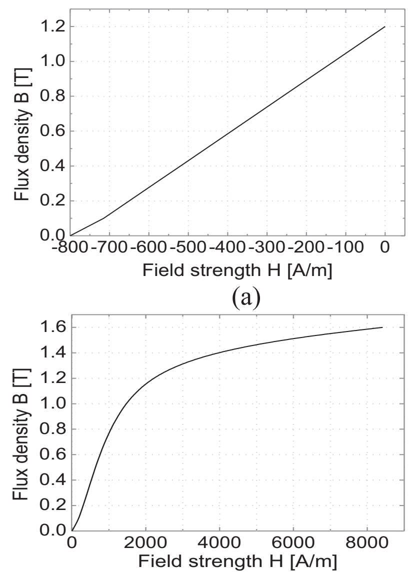

Fig. 3. B-H curves used in FEA: (a) NdFeB, (b) SMC material, Somaloy 700.

Figure 4 (a) to (c) shows the 2-D FEA predicted open-circuit magnetic flux distributions of the three proposed TLPMM designs, with quasi-Halbach magnetized armatures at the maximum armature displacement (z_d = 11 mm) and zero armature current. As can be seen, at the maximum stroke position, most of the flux from the PMs flows through the teeth and back iron, and the flux-linkage with the coil is at the maximum value. The flux is dominant in the radial direction. The resulting flux density in the tooth region varies with time as the armature reciprocates. The flux passing through the yoke is the same as in the teeth. However, the resulting flux density components in the yoke region is essentially in the axial direction.

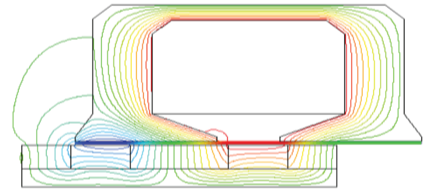

(a)

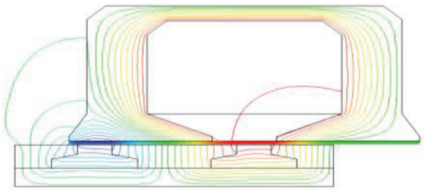
(b)

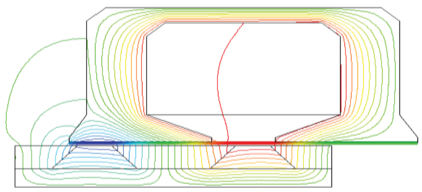
(c)

Fig. 4. Magnetic flux distribution in the three TLPMMs at z_d = 11 mm: (a) flux-lines of Rec_PMs, (b) flux-lines of TS_PMs, and (c) flux-lines of Trap_PMs.

To compare the performances of the three designs, the simulation results of the open-circuit magnetic field were established at the air gap of the motors.

Figure 5 shows the comparison among the magnetic flux distribution at the air gap of the three designs. All results have been shown at z_d = 0 mm. From Fig. 5, we can note that the maximum magnetic flux values were 0.18 mwb/m, 0.16 mwb/m and 0.17 mwb/m for the Rec_PMs, TS_PMs and Trap_PMs, respectively. The TLPMM with Trap_PM showed a higher average value for the air gap magnetic flux, which is conducive to a larger actuating force as compared with the conventional TLPMM design with Rec_PMs. Apparently, the waveform of the magnetic flux was very close to sinusoidal; subsequently, the induced voltage can be quantified by the waveform of the magnetic flux, and was most probably sinusoidal.

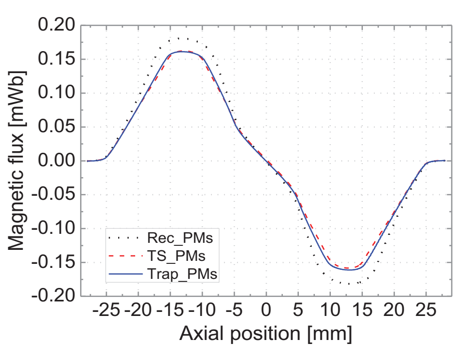

Fig. 5. Comparison between the magnetic flux distributions at the air gap of the three proposed designs.

Figure 6 compares the FEA calculation of the radial magnetic flux density, B_r, in the air gap of the three TLPMM designs as a function of the axial position without an excitation current. At the initial position of the translator, it was found that the higher average value of the air gap flux density was obtained for the proposed design with Trap_PMs. The second maximum average was found for the proposed design with TS_PMs.

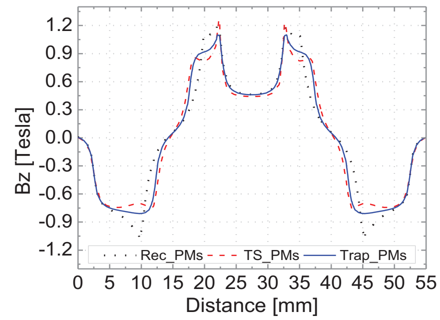

Fig. 6. Comparison of the air gap magnetic flux density components of the three designs.

The no-load magnetic field distribution was calculated using the FEA in order to find out the magnetic flux-linkage of the three designs. The displacement was generated from the forth and back movements of the motor.

The maximum flux-linkage was obtained for the TLPMM with Trap_PMs, while the TLPMM with Rec_PMs showed the lower flux-linkage in the group as represented in Fig. 7. The average value of the flux-linkage with the windings were found to be as in Table 2.

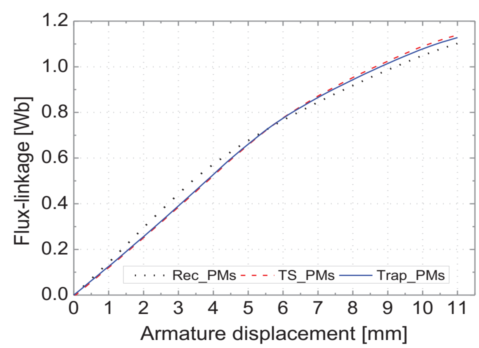

Fig. 7. Comparison of the flux-linkage of the three proposed designs.

Table 2: Average flux-linkages of the three designs

TLPMM	Rec_PMs	TS_PMs	Trap_PMs
Flux-linkage	0.6595 Wb	0.6568 Wb	0.6553 Wb

Figure 8 compares the back-EMF waveforms of the three designs. The armature translated at a mover velocity of 2.2 m/s; whereas, at the zero speed of the motor, the induced voltage was very small or zero. The average values of the back-EMFs for three proposed designs were calculated by 2-D FEA as in Table 3. Obviously, the flux-linkages and back-EMFs of the T-shaped PMs and trapezoidal-shaped PMs were superior to the rectangular-shaped PMs design.

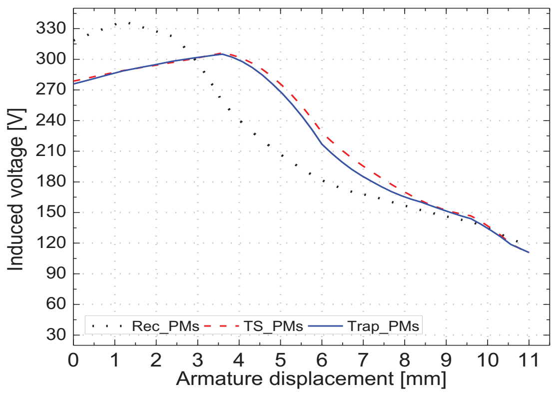

Fig. 8. Comparison of the back-EMFs of the three TLPMMs.

Table 3: Average back-EMFs of the three designs

TLPMM	Rec_PMs	TS_PMs	Trap_PMs
Back-EMF	215.0048 V	223.8931 V	220.3778 V

By passing the current $i_a = 0.5$ A into the stator coil, the reciprocating thrust force yielded as a result of the interaction between the PM field and the current of the coil, also the thrust force depended on the displacement of the PM armature. Figure 9 compares the FE simulation results of the thrust forces of the three proposed TLPMMs. The average thrust forces were quantified as 72.798 N, 83.253 N and 85.185 N for the Rec_PMs, TS _PMs and Trap _PMs, respectively.

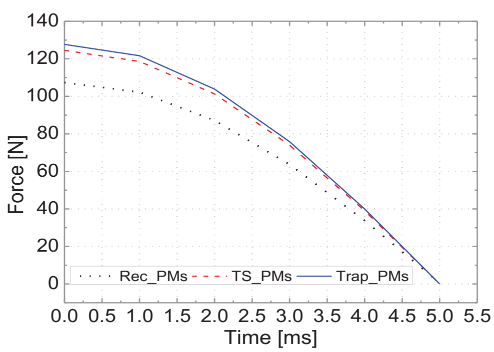

Fig. 9. Comparison of the thrust force of the three TLPMMs.

Winding inductance represents one of the key parameters for the motor performance. Figure 10 compares the calculated winding inductances of the three designs at different displacements of the mover using 2D-FEA. The average values were found to be 716.9721 mH, 751.8687 mH and 753.8792 mH for the TLPMM with Rec_PMs, TS_PMs and Trap_PMs, respectively.

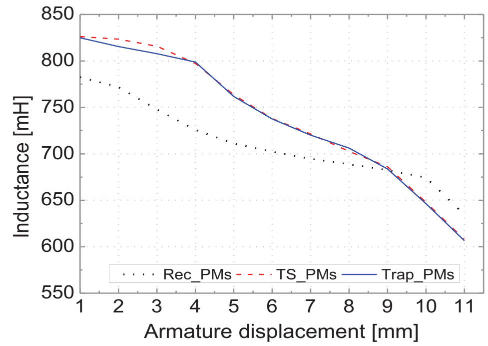

Fig. 10. Comparison of the winding inductances of the three designs.

V. CONCLUSION

In this paper, three designs of tubular linear permanent magnet motors (TLPMMs) were proposed and a 3D-FE model was developed for each one. These motors are proposed to drive a vapor linear reciprocating compressor in a household refrigerator. The three designs have different PM structures; they are the rectangular-shaped PMs (Rec_PMs), trapezoidal-shaped PMs (Trap_PMs) and T-shaped PMs (TS_PMs). These designs have been equipped with a quasi-Halbach magnetized moving-magnet armature and slotted stator with a single coil. The stator cores of all designs have been made of a soft magnetic composite (SMC) material, Somaloy 700; whereas, the PMs were made of NdFeB. Based on the nonlinear 2D-FEA, the results of the proposed designs have been established and compared which ensures an efficient operation of the proposed TLPMMs. The simulation results reveal that the proposed TLPMM with the T-shaped PMs and trapezoidal-shaped PMs are superior to the design with conventional rectangular-shaped PMs, in terms of flux-linkage, back-EMF, force capability, inductance and air gap magnetic field distributions. Subsequently, the simulation results have demonstrated the validity of the designs in driving the linear vapor reciprocating compressor. The prototype of the trapezoidal-shaped PM TLPMM has been fabricated and its testing will be presented in the coming publications.

ACKNOWLEDGMENT

The authors would like to thank University Teknologi PETRONAS (UTP), Malaysia and the Ministry of Education, Malaysia, for the financial support.

REFERENCES

[1] J. Wang and D. Howe, “Tubular modular permanent-magnet machines equipped with quasi-Halbach magnetized magnets-part I: magnetic field

distribution, EMF, and thrust force," *IEEE Trans. on Magnetics*, vol. 41, pp. 2470-2478, 2005.

[2] I. I. Abdalla, T. Ibrahim, and N. Nor, "Linear permanent magnet motor for reciprocating compressor applications," *IEEE 7th Int. Power Engineering and Optimization Conference, PEOCO*, pp. 29-34, 2013.

[3] B. J. Ruiz-Mendoza and C. Sheinbaum-Pardo, "Electricity sector reforms in four Latin-American countries and their impact on carbon dioxide emissions and renewable energy," *Energy Policy*, vol. 38, pp. 6755-6766, 2010.

[4] H. Dai, T. Masui, Y. Matsuoka, and S. Fujimori, "The impacts of China's household consumption expenditure patterns on energy demand and carbon emissions towards 2050," *Energy Policy*, 2012.

[5] J. Wang, D. Howe, and Z. Lin, "Comparative studies on linear motor topologies for reciprocating vapor compressors," *IEEE Int. Conf.* in *Electric Machines & Drives, IEMDC*, pp. 364-369, 2007.

[6] P. Binneberg, E. Kraus, and H. Quack, "Reduction in power consumption of household refrigerators by using variable speed compressors," *Int. Refrigeration and Air Conditioning Conf*., 2002.

[7] M. L. Stoop and A. J. Lambert, "Processing of discarded refrigerators in the Netherlands," *Technovation*, vol. 18, pp. 101-110, 1998.

[8] J. M. Calm and D. A. Didion, "Trade-offs in refrigerant selections: past, present, and future," *International Journal of Refrigeration*, vol. 21, pp. 308-321, 1998.

[9] S. Hou, H. Li, and H. Zhang, "An open air–vapor compression refrigeration system for air-conditioning and desalination on ship," *Desalination*, vol. 222, pp. 646-655, 2008.

[10] J. Wang, D. Howe, and Z. Lin, "Design optimization of short-stroke single-phase tubular permanent-magnet motor for refrigeration applications," *IEEE Trans. on Industrial Electronics*, vol. 57, pp. 327-334, 2010.

[11] J. Wang, D. Howe, and Z. Lin, "Analysis of a short-stroke, single-phase, quasi-Halbach magnetised tubular permanent magnet motor for linear compressor applications," *IET Electric Power Applications*, vol. 2, pp. 193-200, 2008.

[12] J. Wang, T. Ibrahim, and D. Howe, "Prediction and measurement of iron loss in a short-stroke, single-phase, tubular permanent magnet machine," *IEEE Trans. on Magnetics*, vol. 46, pp. 1315-1318, 2010.

[13] Z. Lin, J. Wang, and D. Howe, "A resonant frequency tracking technique for linear vapor compressors," *IEEE Int. Conf. in Electric Machines & Drives, IEMDC*, pp. 370-375, 2007.

[14] Y.-M. Chen, S.-Y. Fan, and W.-S. Lu, "Performance analysis of linear permanent-magnet motors with finite-element analysis," *IEEE Trans. on Magnetics*, vol. 44, pp. 377-385, 2008.

[15] I. I. Abdalla, T. Ibrahim, and N. Mohd Nor, "Analysis of a tubular linear permanent magnet motor for reciprocating compressor applications," *Applied Mechanics and Materials*, vol. 448, pp. 2114-2119, 2014.

[16] T. Ibrahim, "Short-stroke, single-phase tubular permanent magnet motors for refrigeration applications," *The University of Sheffield*, 2009.

[17] J. F. Gieras, Z. J. Piech, and B. Tomczuk, *Linear Synchronous Motors: Transportation and Automation Systems*, CRC Press, 2011.

[18] J. R. Brauer, *Magnetic Actuators and Sensors*, John Wiley & Sons, 2006.

[19] J. Pyrhönen, T. Jokinen, and V. Hrabovcová, *Design of Rotating Electrical Machines*, Wiley Online Library, 2009.

Izzeldin Idris Abdalla was born in Kordofan Province, Sudan, in 1982. He received his B.Sc. (Hons.) degree and M.Sc. in Electrical and Electronic Engineering, specializing in Power and Energy from Juba University, Sudan in the year 2005 and Universiti Teknologi PETRONAS, Malaysia in 2011, respectively. He was in the faculty of Engineering, Department of Electrical and Electronic Engineering, Juba University from 2005 to 2008. He joined Department of Electrical and Electronic Engineering, Universiti Teknologi PETRONAS, Malaysia in January 2012 as a Ph.D. student. His areas of interests are in power electronics, power systems and power quality. His current research interests are in analysis and design of electrical machines.

Taib Ibrahim was born in Kedah, Malaysia in 1972. He received the B.Eng. (Hons) in Electrical and Electronics Engineering, M.Sc. in Electrical Power Engineering and Ph.D. in Electrical Machine Design from Coventry University, U.K. in 1996, University of Strathclyde, UK in 2000 and University of Sheffield, UK in 2009, respectively. His employment experience includes Airod (M) SdnBhd and Universiti Teknologi PETRONAS (UTP). Currently, he is Leader for Power and Energy Cluster and Member for Mission Oriented Research (Energy) in UTP. His research interests range from motion control to electromagnetic devices and their associated drives.

Nursyarizal Mohd Nor obtained his Ph.D. in Electrical Engineering from Universiti Teknologi PETRONAS (UTP), Malaysia in year 2009. In year 2001 he obtained his M.Sc. in Electrical Power Engineering from The University of Manchester Institute of Science and Technology (UMIST), UK. His areas of specialization are 'Analysis and optimization of large scale power systems' and 'State estimation'. He has several publications at his credit. His research interests are in Power Economics Operation and Control, Power Quality and Power System Analysis.